

Finite Element Modeling and Analysis in estimation of air-gap torque of Induction Machine using Arkkio's method

Ravi J Kumar*

* Faculty of Electrical Engineering
Usha Rama College of Engineering & Technology
Andhra Pradesh, INDIA.

Basavaraja Banakara**

** Faculty of Electrical Engineering
University BDT College of Engineering
Karnataka, INDIA.

Abstract— This paper presents electromagnetic and thermal behavior of Induction Motor (IM) through the modeling and analysis by applying multiphysics coupled Finite Element Analysis (FEA). The prediction of the magnetic flux, electromagnetic torque, stator and rotor losses and temperature distribution inside an operating electric motor are the most important issues during its design. Also prediction of these issues allows design engineers to estimate whether the machine is capable for the proposed application and its temperature class for which it is being designed ensuring normal motor operation at rated conditions. In this work, multiphysics coupled electromagnetic – thermal modeling and analysis of induction motor at rated and high frequency has carried out applying Arkkio's torque method. Numerical modeling and finite element analysis carried using COMSOL Multiphysics software. Transient electromagnetic torque, magnetic field distribution, speed-torque characteristics of IM were plotted and studied at different frequencies. This proposed work helps in the design and prediction of accurate performance of induction motor specific to various industrial drive applications. Results obtained are also validated with experimental analysis. The main purpose of this model is to use it as an integral part of the design aiming to system optimization of Variable Speed Drive (VSD) and its components using coupled simulations.

Keywords— *Induction motor, variable speed drive, finite element analysis, electromagnetic torque, Arkkio's method multiphysics, COMSOL Multiphysics and coupled simulations.*

I. INTRODUCTION

Induction motors are vital in various low voltage (LV) and medium voltage (MV) traction, process, oil and gas applications. Voltage source inverter (VSI) became popular in speed control of the induction motor because of its voltage and frequency control capabilities. There are not only advantages but also few disadvantages with VSI's. Since these VSI's inject various odd order harmonics, performance of induction motor has become unpredictable in the VSD applications.

Accurate calculation of various motor parameters is very important in the design of VSD specific to the application. This is because of non-sinusoidal harmonics rich supply generated by high frequency switching devices used in VSI [2]. Since IM performance is different for sine and non-sinusoidal supply, these accurate predictions aids in the effective design of VSI

fed MV and HV IMs. Space and time harmonics developed due to various design considerations of IM affects its air-gap flux, electromagnetic torque and also loading capability of the VSD along with odd order harmonics generated by switching devices. These harmonics induces extra eddy currents in the stator steel and other metal parts of IM by seriously damaging winding and stator slot insulation. Above discussed points are some of vital reasons for increase of down time of VSD in various critical applications like chemical, oil and gas process. Some researches already exist in the LV IM modeling, mostly based on analytical numerical techniques as presented in [5] and [6]. Use of Finite Element Method (FEM) in the modeling and analysis of nonlinear electric devices helps in precise prediction of various electrical parameters rather than use of traditional modeling techniques. FEM aids for quantitative determination of the effect of every single parameter on the dynamical performance of the machine.

This work presents coupled electromagnetic thermal 2D FEM model of IM to simulate its electromagnetic and thermal behavior during the transient duty towards steady-state operation at rated load. Also the main aim of proposed work is to accurately estimate electromagnetic torque in the air gap, temperature distribution in the motor parts; significant displacement currents may run across the stator insulation and bearing currents as input for optimization of efficiency of VSD using coupled simulations.

II. NUMERICAL SOLUTION

It is relatively modest to employ the magnetic vector potential in the numerical solution of the field the induction motor since its simplicity to represent the magnetic fields as a two-dimensional model. Due to complex structure of induction motor, fields of the machine are clearly three dimensional, that's why a two-dimensional solution is always close approximation.

In the 2D modeling of induction motor [1] and [3],

A. Maxwell Equations

Let us start with the application of full three-dimensional vector equations.

The magnetic vector potential A is given by

$$\mathbf{B} = \nabla \times \mathbf{A} \quad (1)$$

Coulomb's condition, required to define explicitly the vector potential, is written as

$$\nabla \cdot \mathbf{A} = 0 \quad (2)$$

The substitution of the definition for the magnetic vector potential in the induction law yields

$$\nabla \times \mathbf{E} = -\nabla \times \frac{\partial \mathbf{A}}{\partial t} \quad (3)$$

Electric field strength can be expressed by the vector potential A and the scalar electric potential ϕ as

$$\mathbf{E} = -\frac{\partial \mathbf{A}}{\partial t} - \nabla \phi \quad (4)$$

' ϕ ' is the reduced electric scalar potential.

Since $\nabla \times \nabla \phi = 0$, adding a scalar potential causes no problems with the induction law. Above equation gives that the electric field strength vector comprises of two parts, they are a rotational part induced by the time dependence of the magnetic field, and a non-rotational part produced by electric charges and the polarization of dielectric materials.

Current density depends on the electric field strength.

$$\mathbf{J} = \sigma \mathbf{E} = -\sigma \frac{\partial \mathbf{A}}{\partial t} - \sigma \nabla \phi \quad (5)$$

Ampere's law and the definition for vector potential gives

$$\nabla \times \left(\frac{1}{\mu} \nabla \times \mathbf{A} \right) + \sigma \frac{\partial \mathbf{A}}{\partial t} + \sigma \nabla \phi = 0 \quad (6)$$

By substituting equation (5) into (6) gives

$$\nabla \times \left(\frac{1}{\mu} \nabla \times \mathbf{A} \right) = \mathbf{J} \quad (7)$$

Equation (7) is valid in zones where eddy currents may be induced, while the equation (6) is valid in zones with source currents $\mathbf{J} = \mathbf{J}_s$, such as stator or rotor winding currents, and in zones without any current densities usually $\mathbf{J} = 0$.

In electrical machines of any type, a 2D solution is often the apparent one as in [1]; in these cases, the numerical solution can be deduced based on a single component of the vector potential A . The solution for fields \mathbf{B} , \mathbf{H} are found in an x-y plane, whereas \mathbf{J} , \mathbf{A} and \mathbf{E} involve only the z-component. The gradient $\nabla \phi$ has a z-component, since \mathbf{J} and \mathbf{A} are parallel to z, and equation (5) is effective. The summarized scalar potential is thus independent of x- and y-components. ' ϕ ' could be a linear function of the z-coordinate, since a 2D field solution is independent of z. The assumption of two-dimensionality is not valid for potential differences caused by electric charges or by the polarization of insulators [4]. For two-dimensional cases with eddy currents, the scalar potential has to be set as $\phi = 0$.

In a 2D case, the equation (6) is rewritten as

$$\nabla \cdot \left(\frac{1}{\mu} \nabla A_z \right) + \sigma \frac{\partial A_z}{\partial t} = 0 \quad (8)$$

Exterior of the eddy current zones, below equation is more valid:

$$-\nabla \cdot \left(\frac{1}{\mu} \nabla A_z \right) = J_z \quad (9)$$

The definition of vector potential provide below components for flux density:

$$B_x = \frac{\partial A_z}{\partial y}; \quad B_y = -\frac{\partial A_z}{\partial x} \quad (10)$$

Therefore, the vector potential remains constant in the direction of the flux density vector.

In the 2D case, the below equation can be obtained from the partial differential equation (PDE) of the vector potential:

$$-k \left[\frac{\partial}{\partial x} \left(\nu \frac{\partial A_z}{\partial x} \right) + \frac{\partial}{\partial y} \left(\nu \frac{\partial A_z}{\partial y} \right) \right] = k J \quad (11)$$

Where ' ν ' is the reluctivity of the material above equation is exactly similar to the equation of a static electric field.

$$\nabla \cdot (\nu \nabla A) = -J \quad (12)$$

B. Boundary Conditions

Definition of two types of boundary conditions for this type of 2D problems is valid. First, Dirichlet's boundary condition indicates that a known potential, so that vector potential

$$A = \text{constant}, \quad (13)$$

This can be attained for a vector potential for example on the outer surface of an electrical induction machine. Since the field is parallel to the contour of the surface. Same as the outer surface of an electrical induction machine, the center line of the machine's pole can develop a symmetry plane. Neumann's homogeneous boundary condition determined with the vector potential

$$\frac{\partial A}{\partial n} = 0 \quad (14)$$

is a second boundary condition accomplished at an instance the field meets a contour perpendicularly. In equation (14) ' \mathbf{n} ' is the normal unit vector of a plane. A contour of this kind is part of a field confined to infinite permeability iron as shown in figure.1. The magnetic flux piercing a surface is easy to determine with the vector potential. Stoke's theorem develops the flux equation.

$$\Phi = \int_S [\mathbf{B} \cdot d\mathbf{S}] = \int_S [(\nabla \times \mathbf{A}) \cdot d\mathbf{S}] = \int_l A \cdot d\mathbf{l} \quad (15)$$

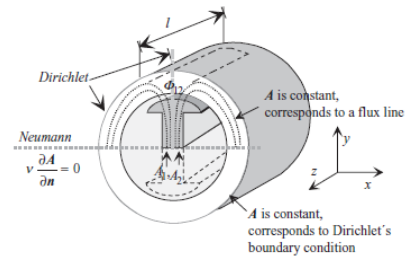


Fig.1. Definition of boundary conditions

Flux ‘ Φ ’ is an integral around the contour ‘ l ’ of the surface S as illustrated in the figure.1. In the 2D case of the illustration [1], the end faces’ part of the integral is zero and the vector potential along the axis is constant.

Consequently, for an induction machine of the length ‘ l ’ we obtain a flux

$$\Phi_{12} = l (A_1 - A_2) \quad (16)$$

This represents that the flux Φ_{12} is the flux between vector equipotential lines A_1 and A_2 .

C. Arkkio’s Torque

Applying finite element assumptions, torque can be determined by differentiating the magnetic co energy W_1 with respect to movement, and by maintaining the winding current constant:

$$T = l \frac{dW_1}{d\alpha} = \frac{d}{d\alpha} \int_v \int_0^H [B \cdot dH] dV \quad (17)$$

In numerical modeling, this air-gap magnetic field energy and torque produced due to it is approximated by the difference between two successive fields.

$$T = (l (W'(\alpha + \Delta\alpha) - W'(\alpha)) / \Delta\alpha \quad (18)$$

Where ‘ l ’ is the machine length and $\Delta\alpha$ represents the displacement between successive field solutions.

There are four different methods to calculate torque of rotating electrical machines using FE modeling; they are Coulomb’s method, Maxwell Tensor method, Magnetic co energy derivation and Arkkio’s method. Among them Arkkio’s method [3] is used in this work to determine torque of IM using FEM. It is a variant of Maxwell’s stress tensor method and is based on integrating the torque over the whole volume of the air gap constituted by the zones of radii r_s and r_r . Torque expression of same is as shown below (19).

$$T = \frac{l}{\mu_0(rs-rr)} \int_s r B_n B_{tan} dS \quad (19)$$

Where l is the length, B_n and B_{tan} represents the radial and tangential flux densities in the elements of surface S and formed between radii rr and rs . dS is the surface of single element.

III. FE MODEL OF IM

Use of Finite element method (FEM) in new era engineering modeling problems and it has become popular due to its capability to solve 2D and 3D engineering problems accurately than previous classical computing techniques.

In this work induction machine modeling is proposed using FEM by applying Arkkio’s method [3]. FEM model of induction motor was developed in the multiphysics modeling software as shown in Figure 2. Definition of parameters, boundary conditions, dimensions of parts of the induction machine is important in FEM model. Definition of moving mesh for the air-gap and moving parts of induction machine yields accurate solution. In this proposed 2D induction machine model electromagnetics and boundary conditions are defined and applied with below Maxwell and Ampere’s law equations from (1) – (14).

Induction motor simulated is constructed as 36 slots, four pole machine. All domains as shown in Fig.3 are defined as triangular elements and both rotor and shaft are defined as boundary layers in order to define them as moving meshes. In this FEM simulation total number of degrees of freedom solved is 28,863. Materials assigned to various sectors of motor under consideration are air gap as air, rotor outer sector defined as aluminum and shaft as steel. Stator coils are defined as solid copper with 2045 number of turns, conductivity of 6×10^7 S/m and cross sectional area as 1×10^{-6} m². Induction motor stator windings are excited with three phase sinusoidal current excitation. Coils are excited with two different frequencies 50Hz and 500Hz in order to observe the difference in the torque development. This gave good insight to the future work to be carried in order to predict and optimize performance of VSD [7] i.e. for system optimization of VSD using coupled simulations. Also thermal and heat transfer behaviors of different sectors existing in the model are defined [9] and coupled with the electrical machine rotating magnetic behavior to accurately determine losses in inverter supplied [8] machine’s performance and electromagnetic torque.

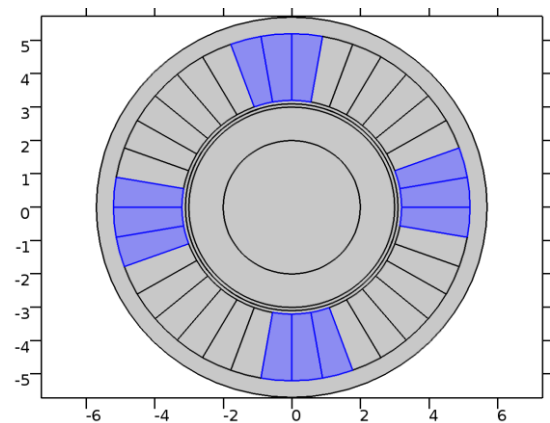


Fig.2. 2D model of induction motor with phase-A coil

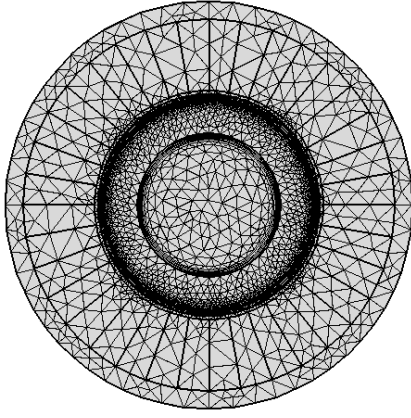


Fig.3. Definition of meshing in different zones

TABLE.1 DEFINITION OF PARAMETERS IN THE DESIGN OF INDUCTION MOTOR

S.No	IM Parameters		
	Parameters	Value	Units
1	Length of the motor	1	m
2	Phase span of a winding	10	deg
3	Outer radius of rotor steel	2	cm
4	Number of turns	2045	
5	Inner radius of windings	3.2	cm
6	Outer radius of rotor aluminum	3	cm
7	Inner radius of stator steel	5.2	cm
8	Outer radius of stator steel	5.7	cm
9	Air gap	0.2	cm

IV. AIR GAP OPTIMIZATION

Optimization of air-gap performed using parametric sweep. Air-gap length is very important parameter which needs to be properly designed to get required torque and performance from the induction machine. It also helps engineers to design proper thickness of slot insulation since it indirectly influences the surface temperatures of the machine. Parametric sweep on air-gap has performed in a range of 0.001m – 0.008m and found that 0.002m-0.004m as the optimal for better performance of the machine. Indeed this parametric sweep has contributed for optimization of machine performance and torque by considering correct thickness of air-gap. These observations and analysis will be utilized in the further work related to optimization of VSD system performance. Various physics interface applied to the model are rotating machinery, electric circuits, heat transfer in solids and differential equations [10]. Results obtained are close to the standard induction motor characteristics at different frequency excitations. This can also be used to optimize various performance characteristics of the machine.

V. ANALYSIS AND RESULTS

The results of the validation using time dependent simulation shows characteristics of magnetic flux density, current density and surface temperature of 4 Pole, 10kW, 36 slot classical Induction Motor operating at 50Hz and 500Hz supply respectively. Stator coils of induction motor are excited with sinusoidal current excitation of 1Amp. Number of turns per slot chosen is 2045 in order to study magnetic flux density and electromagnetic torque at highly enclosed induced e.m.f around coils.

A. Magnetic flux density and Current density

Post processing of the proposed time dependent study at 50Hz and 500Hz supply depicts various interesting results of uniform magnetic flux density, current density as shown in Fig 4 and 5. Load torque applied was a step of 4Nm and simulation time set as 0.8 sec to study transient behavior of the induction motor. Results depicts that no much difference in the magnetic flux density at 50Hz and 500Hz operations while current density norm has got in to wide variation at 500Hz operation. This is very important to predict in the design phase in order to decide the appropriate air gap and other dimensions of the machine.

B. Electromagnetic Torque

Different frequencies 50Hz and 500Hz are considered to cross check accuracy of electromagnetic torque development as shown in Fig.7a & 7b by the induction motor, it was observed that torque developed exactly matches with standard characteristics in both cases.

C. Thermal Analysis

Heat development and distribution in the stator core by heat sources during starting was more at lower frequencies than at higher frequencies. Stator winding, rotor cage are defined as heat sources to plot thermal analysis. Thermal analysis plots Fig 6a & 6b shows clearly intensity of heat during starting at two different operations.

D. Speed-Torque characteristics

Angular speed and speed-torque characteristics shown in Fig. 8 & 9 are better than obtained by analytical methods. Estimation of speed-torque characteristics very important to decide switching pulses and control strategies required for specific VSD applications. From Fig. 8a & 8b, it is clear that rise of speed of cage rotor induction motor is accurate and standard at starting for an applied step torque of 4Nm. This helps to decide appropriate soft starting technique, especially in flammable atmospheres where rise of surface temperatures are controlled by various global standards to avoid auto ignition of flammable vapors.

E. Electric displacement and Current density in stator core

From plots in Fig. 10a & 10b it is observed that electric displacement variation is drastic in the same material from 50Hz to 500Hz which need to be considered in the design of insulation class and thickness of insulation. As we know that the displacement current is insignificant from the viewpoint of the machine's basic functionality. However, when a motor is excited by a frequency converter and the high frequencies created switching devices lead to significant displacement currents may run across the insulation and bearing current problems. So, prediction of electric displacement and current density provides vision for accurate design of insulation class.

Firstly, the review and analysis of several characteristics of proposed cage rotor induction motor, one should understand the importance to predict the performance of IM prior to it's loading in countless industrial applications. Secondly, precise numerical estimation of above complex geometry parameters aids design engineers to appropriately select control drive to be coupled and used in many VSD applications. Finally, type and thickness of insulation, time setting of thermal relays used in the protection of MV and HV machines can be predicted to optimize the performance of the cage rotor induction motors.

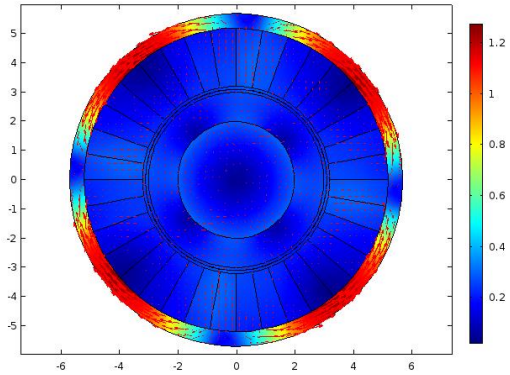


Fig.4a. Surface Magnetic flux density in the material (T) at $f=50\text{Hz}$

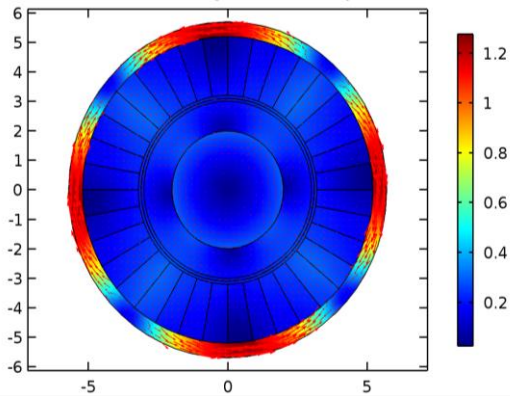


Fig.4b. Surface Magnetic flux density in the material (T) at $f=500\text{Hz}$

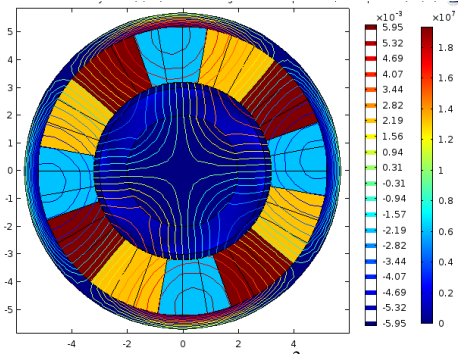


Fig.5a. Current density norm (A/m^2) and Magnetic vector potential, z component (Wb/m) at $f = 50\text{Hz}$

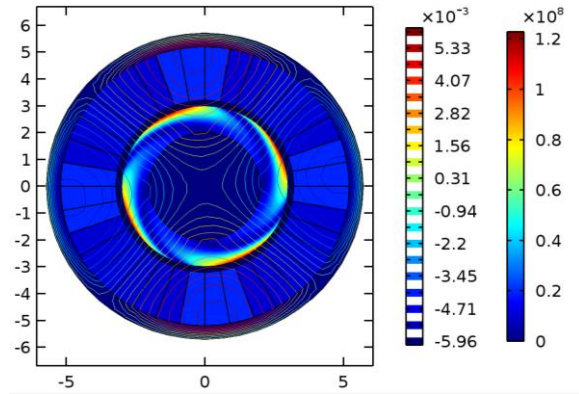


Fig.5b. Current density norm (A/m^2) and Magnetic vector potential, z component (Wb/m) at $f = 500\text{Hz}$

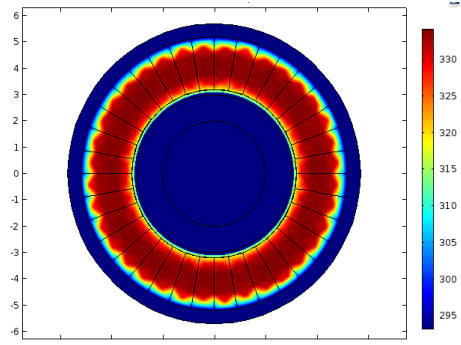


Fig.6a. Surface temperature (K) at $f=50\text{Hz}$

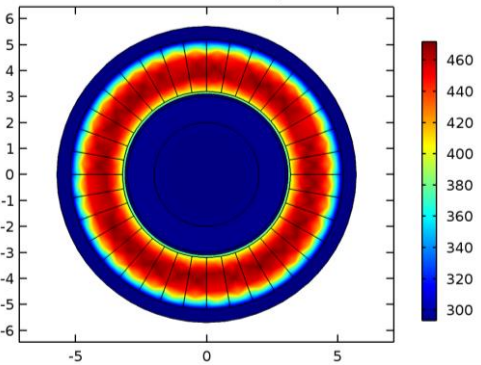


Fig.6b. Surface temperature (K) at $f=500\text{Hz}$

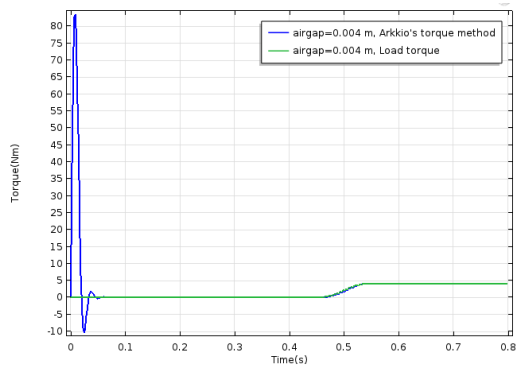


Fig.7a. Electromagnetic torque (Nm) at $f=50\text{Hz}$

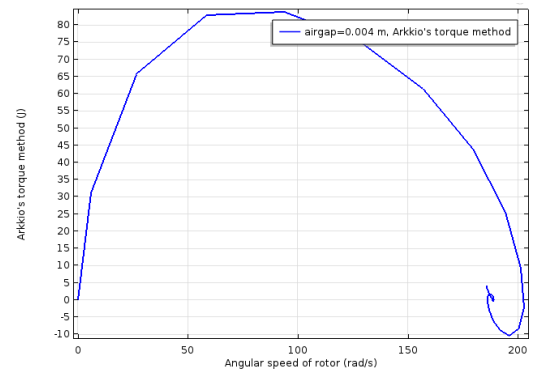


Fig.9a. Speed-Torque characteristics at $f=50\text{Hz}$

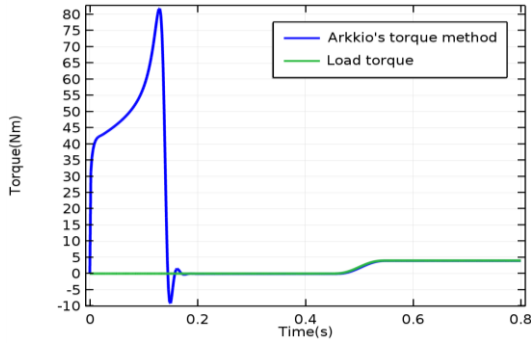


Fig.7b. Electromagnetic torque (Nm) at $f=500\text{Hz}$

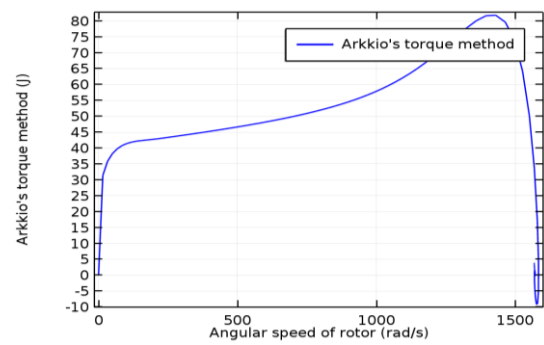


Fig.9b. Speed-Torque characteristics at $f=500\text{Hz}$

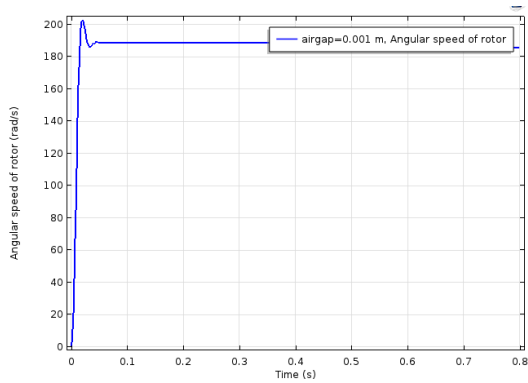


Fig.8a. Angular speed of rotor (rad/sec) at $f=50\text{Hz}$

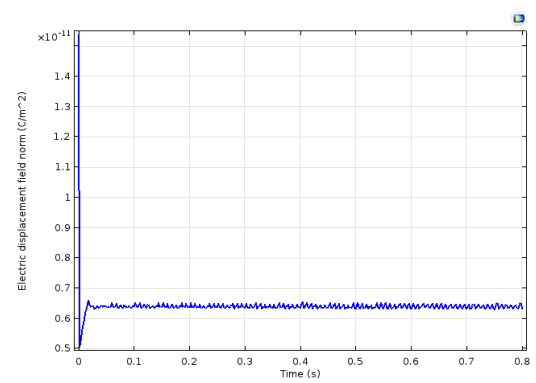


Fig.10a. Electric displacement, D (C/m^2) in stator core at $f=50\text{Hz}$

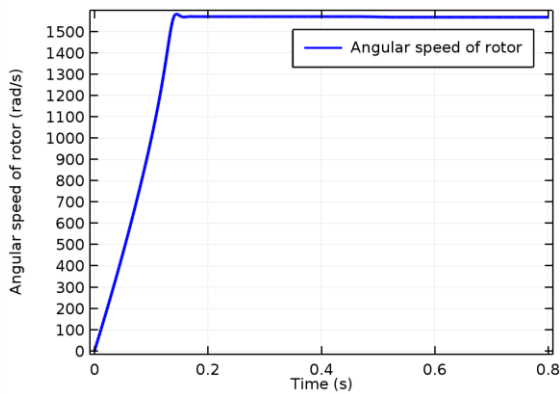


Fig.8b. Angular speed of rotor (rad/sec) at $f=500\text{Hz}$

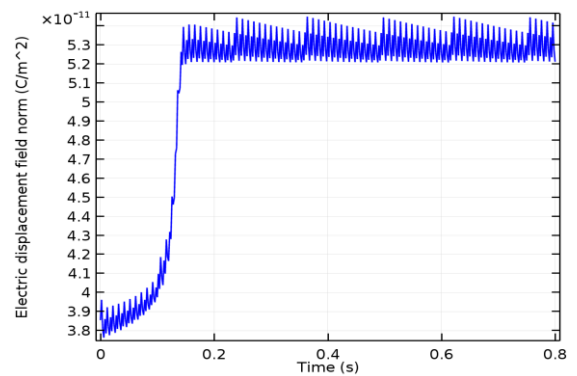


Fig.10a. Electric displacement, D (C/m^2) in stator core at $f=500\text{Hz}$

VI. CONCLUSIONS

This paper has described the development of a coupled thermal-electromagnetic model for accurate estimation of electromagnetic torque and thermal condition of cage-rotor induction motor under standard supply systems at different frequencies. The developed electromagnetic-thermal model is a combination of coupled multiphysics. Arkkio's method is used to model IM using FEM and software used to model is COMSOL multiphysics. Electrical circuit and heat transfer in solids physics are coupled internally in order to develop coupled FEM electromagnetic-thermal IM model. The equivalent circuit parameters of the induction motor under different operating conditions are obtained experimentally to compare with FEM simulation results. These results helps to predict electromagnetic-thermal condition of the motor under standard supply system at different frequencies and the necessary derating of the motor can be carried out prior to application to avoid unexpected breakdown of VSD. The predicted torque, temperature and other characteristics are very close to the experimental results. This model can be very useful to determine the electromagnetic and thermal condition of the motor in many stringent operating conditions. This work is developed as input to the "system optimization of VSD using coupled simulations" which is under research and same will be presented in the future work.

ACKNOWLEDGEMENTS

Authors would like thank Science and Engineering Research Board (SERB), Directorate of Science and Technology (DST), New Delhi, Government of India for funding this project. Authors also like to thank management of Usha Rama College of Engineering and Technology for their

extended support in providing all other facilities required for completion of this project.

REFERENCES

- [1] J. Pyrhönen, T. Jokinen, and V. Hrabovcová, Design of Rotating Electrical Machines. John Wiley & Sons Ltd, 2008.
- [2] M. J. Islam, H. V. Khang, A. K. Repo, and A. Arkkio, "Eddy Current Loss and Temperature Rise in the Form-Wound Stator Winding of an Inverter Fed Cage Induction Motor," *IEEE Trans. on Magnetics*, vol. 46, no. 8, Aug. 2010.
- [3] A. Arkkio, "Analysis of Induction Motors Based on the Numerical Solution of the Magnetic Field and Circuit Equations", Acta Polytechnica Scandinavica, Electrical Engineering Series, No. 59, 1987, p. 97.
- [4] A.M. Oliveira, P. Kuo-Peng, N. Sadowski, M.S. de Andrade, J.P.A Bastos, "A non-a priori approach to analyze electrical machines modeled by FEM connected to static converters", *IEEE Trans. Magn.*, Vol. 38, No. 2, pp. 933–936, 2002.
- [5] S. Kanerva, S. Seman, A. Arkkio, "Simulation of Electric Drive Systems with Coupled Finite Element Analysis and System Simulator", 10th European Conference on Power Electronics and Applications (EPE 2003), Toulouse, France, September 2–4, 2003.
- [6] P Zhou, W.N.Fu, .D.Lin S. Stanton, Z.J.Cendes, "Numerical Modeling of Magnetic Devices", *IEEE Transactions on Magnetics*, Vol.40 No.4, 2004.
- [7] S.Kanerva, C.Stutlz, B.Gerhard, H.Burzanowska, J.Jarvinen, S.Seman "Coupled FEM and System Simulator in the simulation of Asynchronous Motor with direct torque control", Laboratory of Electromechanics, Helsinki University of Technology, HUT, 3000, FI-02015, Finland
- [8] T.C. Green, CA Hernandez-Aramburo and AC. Smith "Losses in grid and inverter supplied induction machine drives" *IEEE Proc. Elec. Power Appl.* Vol.150, No.6, November 2003.
- [9] S. Mezani, N. Takorabet and B Laporte, "A combined electromagnetic and thermal analysis of induction motors", *IEEE transactions on Magnetics*, Vol. 41, No. 5, pp. 1572-1575, May 2005.
- [10] M. J. Duran and J. Fernandez, "Lumped-parameter thermal model for induction machines", *IEEE transactions on Energy Conversion*, Vol. 19, No. 4, pp. 791-792, Dec. 2004.